Journal of chemical & engineering data

Article

pubs.acs.org/jced

Solubility and Induction Period Study of Asiaticoside and Madecassoside in a Methanol + Water Mixture

Xing-Fang Zheng, Jie Fu,* and Xiu-Yang Lu*

Key Laboratory of Biomass Chemical Engineering of Ministry of Education, Department of Chemical and Biological Engineering, Zhejiang University, Hangzhou 310027, China

ABSTRACT: The solubilities of madecassoside in a mixture of methanol + water were determined in the temperature range from (298.15 to 328.15) K by a static analytical method. A "W"-type curve was found for the solubility of madecassoside in the mixture of methanol + water. The induction periods of asiaticoside and madecassoside in a mixture of methanol + water were determined at 298.15 K by a laser scattering method. The results show that the solubilities of madecassoside are similar to those of asiaticoside in the mixture of methanol−water excluding those at high water content and high temperature. However, these two compounds with the only difference of 6-OH exhibit a quite different crystallization property that the induction period of madecassoside is at least 10 times longer than asiaticoside. Moreover, the interfacial tension data of asiaticoside were obtained, which are in the range of (0.55 to 0.86) mJ·m^{-2}.

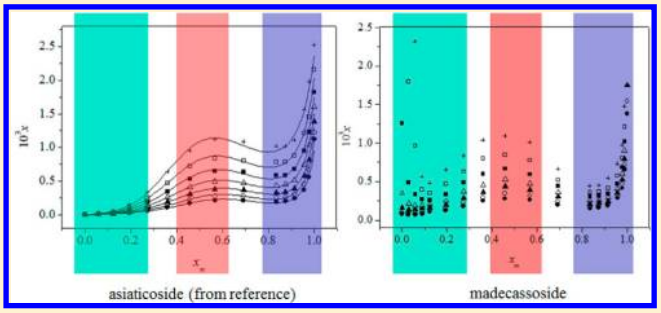

1. INTRODUCTION

The solubility difference is the main driving force in the crystallization separation process, and induction period t_{ind} is defined as the time interval between the start of supersaturation and the formation of critical nuclei.[1,2] It has been often employed as a measurement of the nucleation event and to derive the interfacial tension,[3] which is a crucial parameter involved in the theories of crystal nucleation and growth. The surface entropy factor, a measurement of the roughness degree of the crystal surface, can also be calculated from the interfacial tension. With the surface entropy factor, a crystal's growth is predictable, and the birth and spread growth is to be expected while the surface entropy factor value is among the range of 3 to 5.

In our previous work, a process combining crystallization[4] with chromatography[5−7] to prepare high-purity asiaticoside from *Centella asiatica* has been developed. The active constituents of *C. asiatica* mainly consist of asiaticoside (2,3,23-trihydroxy-*O*-6-deoxy-*α*-L-mannopyranosyl-(1→4)-*O*-*β*-D-glucopyranosyl-(1→6)-*β*-D-glucopyranosyl ester, (2*α*,3*β*,4*α*)-urs-12-en-28-oic acid, CAS Registry No. 16830-15-2, Figure 1) and madecassoside (2,3,6,23-tetrahydroxy-*O*-6-deoxy-*α*-L-mannopyranosyl-(1→4)-*O*-*β*-D-glucopyranosyl-(1→6)-*β*-D-glucopyranosyl ester, (2*α*,3*β*,4*α*,6*β*)-urs-12-en-28-oic acid, CAS Registry No. 34540-22-2, Figure 1), which only have a difference in 6-OH. For investigating the crystallization separation process and studying the mechanism of crystal nucleation and growth in the drawing-out process, there is a need to determine the solubility and induction period[8] of asiaticoside[9,10] and madecassoside.

There is a modest body of literature concerning the nucleation mechanism of small molecules such as inorganic salts, organic salts,[11−15] and proteins.[16] The induction period may be determined either by visual observation, measurement of turbidity, or measurement of any concentration-dependent property which varies sufficiently in the course of the crystallization process[17] such as conductivity,[12,13,18−22] intensity of transmitted or scattered light,[14,23−25] pH,[26] heat re-

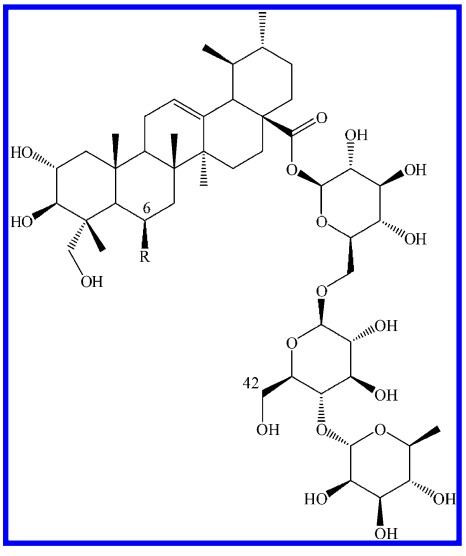

Figure 1. Structural formula of asiaticoside (R = H) and madecassoside (R = OH).

Received: August 7, 2012
Accepted: September 27, 2012
Published: October 5, 2012

Table 1. Sample Table

chemical name	source	initial mass fraction purity	purification method	final mass fraction purity	analysis method
asiaticoside	GCNPD[a]	0.90	recrystallization	0.98	HPLC[d]
madecassoside	GCNPD	0.90	recrystallization	0.98	HPLC
asiaticoside standard	Sigma	> 0.985			
madecassoside standard	STB[b]	0.95			
methanol	SCR[c]	≥ 0.995			
acetonitrile	Merck	≥ 0.999			

[a]Guangxi Changzhou Natural Products Development Co., Ltd. [b]Shanghai Tauto Biotech Co., Ltd. [c]Sinopharm Chemical Reagent Co., Ltd. [d]High-performance liquid chromatography.

leased,[27,28] and activity of precipitated ions.[12] However, to the best of our knowledge, there is no study on the induction period of asiaticoside or madecassoside and their nucleation or crystal growth mechanisms. The experimental solubility of madecassoside is also not available in the literature.

In this study, the induction periods of asiaticoside and madecassoside are determined to disclose the crystallization mechanism of asiaticoside and madecassoside in the methanol−water system. The solubilities of madecassoside in the methanol−water system over the temperature range from (298.15 to 328.15) K, which is important for the induction period research, are also determined. The results provide insights on the crystallization process of these two compounds.

2. EXPERIMENTAL SECTION

2.1. Chemicals. The raw material asiaticoside (0.90 mass fraction purity), obtained from Guangxi Changzhou Natural Products Development Co., Ltd. (Guangxi, China), was recrystallized four times with methanol before use. The raw material madecassoside (0.90 mass fraction purity), obtained from Guangxi Changzhou Natural Products Development Co., Ltd. (Guangxi, China), was also recrystallized four times with methanol−water (0.88, mass fraction of methanol) before use. Then they were dried for 24 h in a vacuum drying oven (323.15 K) to ensure that its mass fraction purity was higher than 0.98 as Table 1 shows.

Asiaticoside standard (> 0.985 mass fraction purity) was purchased from Sigma. Madecassoside standard (0.95 mass fraction purity) was purchased from Shanghai Tauto Biotech Co., Ltd. (Shanghai, China). Analytical reagent (AR) grade methanol (≥ 0.995 mass fraction purity) was obtained from Sinopharm Chemical Reagent Co., Ltd. (Shanghai, China). Distilled water was obtained from Hangzhou Wahaha Group Co., Ltd. (Hangzhou, China). High-performance liquid chromatography (HPLC) grade acetonitrile (≥ 0.999 mass fraction purity) was obtained from Merck (Darmstadt, Germany).

2.2. Solubility Research. The mole fraction solubility x determination in this study was conducted by a static−analytical method described in our previous work.[29−32] A period of 12 h of stirring and 6 h of settling could achieve the reproducibility of the data within 0.5 %, ensuring the achievement of equilibrium. Approximately 1 g of saturated solution was quickly taken out for each test. It was weighed and diluted with the mixture of methanol and water (0.44, mass fraction of methanol) to a certain volume, then analyzed by HPLC (Agilent 1100).

A Synergi 4 μm Hydro-RP 80A reverse-phase column (4.6 mm × 250 mm, 4 μm, Phenomenex) was employed for the analysis. The flow rate was 0.5 mL·min^{-1}; the wavelength was 205 nm, and the column temperature was 298.15 K. The mobile phase was acetonitrile and water at 0.20 mass fraction of acetonitrile. The linear range was (0.0207 to 0.3318) mg·mL^{-1}.

2.3. Induction Period Research. The conductivity method was widely used for the determination of induction period due to its good stability and sensitivity. However, it was claimed that the solute should be electrolyte which has electric conduction nature. Therefore, the scattered light method is adopted to study the induction period of these two triterpenoids. The experimental apparatus for the induction period measurement is shown in Figure 2. A precision water bath, a motorized stirrer, and a 0.2 μm filter were used to reach homogeneous concentration and temperature. The experimental conditions, including the vessel size, type, material of construction, and agitation rate were held constant. A desired amount of solute was dissolved in methanol and maintained at 298.15 K for 12 h. Then a desired amount of the solution was filtered and poured into the crystallizer at an agitation rate of 500 rpm. After the temperature of the solution was steady at 298.15 K and the laser signal remained constant for several minutes, the required amount of filtered water was added into the vessel as soon as possible, and the timer was started at the same time. The laser signal changed with the drawing out nuclei, and the experiment was quenched after the laser signal has no significant change. The time that elapsed between the time point when the water was added, and the change of the laser signal was defined as the induction period.

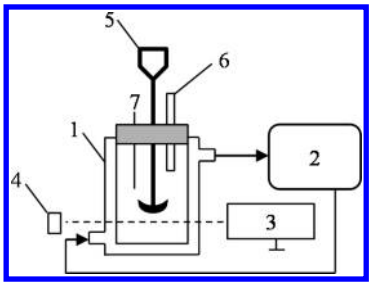

Figure 2. Experimental setup for induction period measurement. (1) crystallizer; (2) water bath; (3) laser generator; (4) laser receiver; (5) motorized stirrer; (6) solvent inlet; (7) thermometer.

The homogeneous primary nucleation rate can be presented as the following classical relation:[3]

$$B = A \exp\left(\frac{16\pi\gamma^3 V_m^2}{3\nu^2 k^3 T^3 \ln^2 S}\right) \quad (1)$$

where B is the nucleation rate, A is a constant, γ is the crystal-solution interfacial tension, V_m is the molecular volume, ν is the moles of ions per mole of electrolyte, k is the Boltzmann constant, T is the absolute temperature, and S is the supersaturation ratio defined by:

dx.doi.org/10.1021/je300883a | J. Chem. Eng. Data 2012, 57, 3258−3263

Table 2. Solubilities of Madecassoside in a Methanol + Water Mixture at Pressure p = 0.1 MPa and Different Temperatures T[a], Together with Error Limits Using the 95 % Confidence Level

	$10^3\ x$					
T/K	x_m = 0	x_m = 0.0288	x_m = 0.0588	x_m = 0.0903	x_m = 0.1233	x_m = 0.1942
298.15	0.0811 ± 0.0002	0.0728 ± 0.00008	0.0735 ± 0.0004	0.0843 ± 0.0002	0.1054 ± 0.0005	0.1278 ± 0.0006
303.15	0.1057 ± 0.0003	0.0882 ± 0.0001	0.0923 ± 0.0005	0.1061 ± 0.0003	0.1283 ± 0.0003	0.1544 ± 0.0005
308.15	0.1607 ± 0.0004	0.1363 ± 0.0006	0.1407 ± 0.0004	0.1499 ± 0.0003	0.1612 ± 0.0002	0.1985 ± 0.001
313.15	0.3494 ± 0.0013	0.2181 ± 0.0010	0.1923 ± 0.0007	0.1933 ± 0.0003	0.2032 ± 0.0003	0.2483 ± 0.0011
314.15	0.7729 ± 0.0042					
318.15	1.2545 ± 0.0081	0.4852 ± 0.0034	0.3364 ± 0.0009	0.2713 ± 0.0008	0.2633 ± 0.0018	0.3372 ± 0.0016
319.15	1.8551 ± 0.0039					
320.15	3.5163 ± 0.0073					
321.15	5.5786 ± 0.0441					
323.15		1.800 ± 0.0132	0.9663 ± 0.0061	0.3965 ± 0.001	0.3537 ± 0.0008	0.4729 ± 0.0034
324.15		3.3017 ± 0.0143				
325.15		4.9101 ± 0.0147				
326.15		6.632 ± 0.0699				
328.15			2.3183 ± 0.0124	0.5638 ± 0.001	0.482 ± 0.0009	0.6491 ± 0.0028
	x_m = 0.2727	x_m = 0.3600	x_m = 0.4576	x_m = 0.5676	x_m = 0.6923	x_m = 0.8351
298.15	0.1818 ± 0.0007	0.2505 ± 0.0009	0.2799 ± 0.0009	0.2646 ± 0.0002	0.2014 ± 0.0008	0.1504 ± 0.0005
303.15	0.2289 ± 0.0004	0.2946 ± 0.0008	0.347 ± 0.0013	0.3139 ± 0.0017	0.2397 ± 0.0009	0.183 ± 0.0008
308.15	0.2854 ± 0.0006	0.3619 ± 0.0011	0.4361 ± 0.0019	0.3928 ± 0.0019	0.3046 ± 0.0021	0.2107 ± 0.002
313.15	0.3752 ± 0.0005	0.4573 ± 0.0016	0.5268 ± 0.0041	0.4731 ± 0.0023	0.3592 ± 0.002	0.2544 ± 0.001
318.15	0.4866 ± 0.0021	0.6006 ± 0.0044	0.6681 ± 0.0036	0.5948 ± 0.0017	0.4461 ± 0.0009	0.3094 ± 0.0008
323.15	0.6311 ± 0.0024	0.7974 ± 0.0049	0.8472 ± 0.0038	0.7766 ± 0.0049	0.5202 ± 0.0114	0.3614 ± 0.0019
328.15	0.8308 ± 0.0036	1.0333 ± 0.0093	1.095 ± 0.0059	1.0108 ± 0.0031	0.6618 ± 0.0017	0.4452 ± 0.0011
	x_m = 0.8740	x_m = 0.9144	x_m = 0.9564	x_m = 0.9780	x_m = 0.9889	x_m = 1
298.15	0.1624 ± 0.0008	0.1927 ± 0.002	0.2887 ± 0.0039	0.4156 ± 0.0032	0.6589 ± 0.0082	1.3826 ± 0.0078
303.15	0.1931 ± 0.0007	0.2117 ± 0.0013	0.3144 ± 0.0024	0.4641 ± 0.0037	0.7163 ± 0.0023	1.5434 ± 0.0114
308.15	0.2238 ± 0.0024	0.2434 ± 0.0021	0.3557 ± 0.0017	0.5246 ± 0.0019	0.7933 ± 0.0061	1.7501 ± 0.0129
313.15	0.2614 ± 0.003	0.2952 ± 0.0011	0.4049 ± 0.0046	0.603 ± 0.0013	0.9049 ± 0.0028	1.7286 ± 0.0028
318.15	0.3142 ± 0.0005	0.3403 ± 0.003	0.4734 ± 0.0033	0.685 ± 0.0037	1.0171 ± 0.003	1.5927 ± 0.0333
323.15	0.3688 ± 0.0012	0.417 ± 0.0018	0.5759 ± 0.0037	0.8035 ± 0.0129	1.2082 ± 0.0073	
328.15	0.4562 ± 0.0034	0.541 ± 0.0014	0.7308 ± 0.0049	0.9743 ± 0.0007	1.4718 ± 0.0034	

[a]Standard uncertainties u are $u(T)$ = 0.05 K.

$$S = \frac{c}{c^*} \tag{2}$$

where c is the initial concentration of solute, and c^* is the equilibrium concentration of solute.

The induction period can be considered as inversely proportional to the nucleation rate as follows:[22]

$$t_{ind}^{-1} \propto B \tag{3}$$

The following equation was obtained by combining eq 1 and taking the logarithm of the induction period:

$$\ln t_{ind} = K + \frac{16\pi\gamma^3 V_m^2}{3\nu^2 k^3 T^3 \ln^2 S} \tag{4}$$

Equation 4 suggests that the plot of ln t_{ind} against $\ln^{-2} S$ should be a straight line for a given temperature. The slope is

$$\alpha = \frac{16\pi\gamma^3 V_m^2}{3\nu^2 k^3 T^3} \tag{5}$$

So, the interfacial tension can be presented by the following equation:

$$\gamma = \left(\frac{3\alpha\nu^2 k^3 T^3}{16\pi V_m^2}\right)^{1/3} \tag{6}$$

3. RESULTS AND DISCUSSION

3.1. Solubilities of Madecassoside. Six samples were taken and analyzed at each tested temperature. The experimental data for the solubilities of madecassoside in a binary mixture of methanol + water at different temperatures are listed in Table 2 with the 95 % confidence level error limits and are also shown in Figure 3.

The results show that the solubilities of madecassoside in a binary mixture of methanol + water increase with temperature. Methanol is a good solvent for madecassoside at all temperatures, which were investigated, although the solubility is smaller than that at high water content and certain temperature (T > 313.15 K). Particularly, while temperature is higher than 308.15 K, yellow powder yielded in the tested solution of madecassoside and the solubility in pure methanol declined as depicted in Figure 4, indicating that madecassoside may be unstable in pure methanol. Moreover, the solubility is sensitive to the water content while methanol mole fraction x_m > 0.956.

The solubility of madecassoside in high methanol content (x_m > 0.1233) is similar to that of asiaticoside, which has been studied in a previous work.[32] At each temperature, the plots exhibit a "W"-type curve, and the solubility is less sensitive to temperature while x_m approaches 0.1233 or 0.8. When x_m = 0.1233 or 0.0903, the solubility of madecassoside is the

dx.doi.org/10.1021/je300883a | J. Chem. Eng. Data 2012, 57, 3258−3263

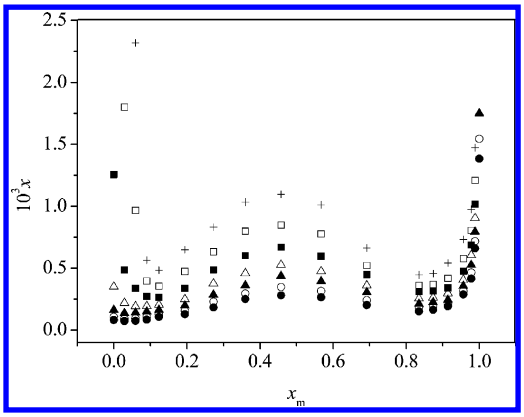

Figure 3. Solubilities x of madecassoside at different temperatures T in the methanol + water mixture as a function of methanol mole fraction x_m. ●, T = 298.15 K; ○, T = 303.15 K; ▲, T = 308.15 K; △, T = 313.15; ■, T = 318.15; □, T = 323.15; +, T = 328.15 K.

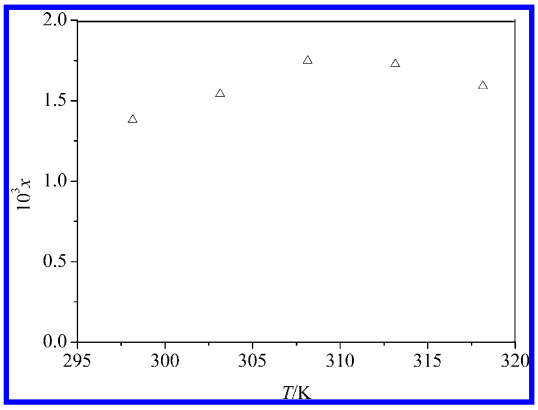

Figure 4. Solubilities x of madecassoside in pure methanol as a function of temperature T.

smallest, but x_m = 0.0903 is more sensitive to high temperature than x_m = 0.1233 as shown in Figure 5. Similarly, in high water

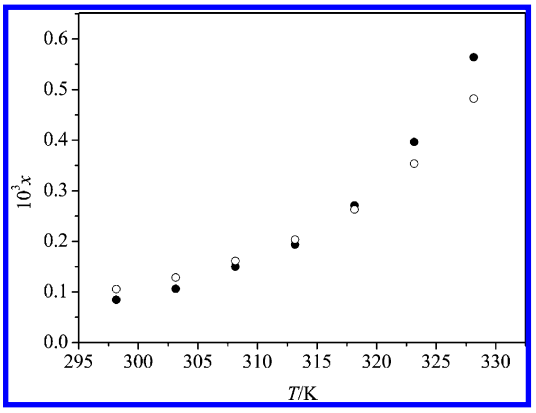

Figure 5. Solubilities x of madecassoside in the methanol + water mixture (x_m, methanol mole fraction) as a function of temperature T. ●, x_m = 0.0903; ○, x_m = 0.1233.

content (x_m < 0.0903) the solubility curve of madecassoside according to the temperature is smooth at low temperature, while it changes near T = 320 K. The solubility in pure water is the most dependent on high temperature, since it has the largest increase in the range of high temperature, as shown in Figure 6.

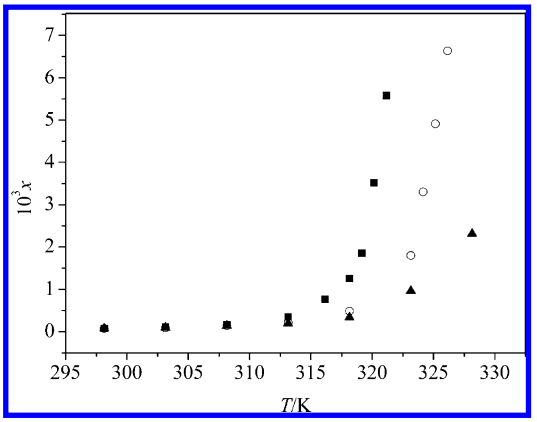

Figure 6. Solubilities x of madecassoside in the methanol + water mixture (x_m, methanol mole fraction) as a function of temperature T. ■, x_m = 0; ○, x_m = 0.0288; ▲, x_m = 0.0588.

The W-type curve may be caused by the effect of methanol–water interactions in the mixed solvent and the specific interactions between the mixed solvent and the madecassoside with a highly polar sugar chain unit.[33] It indicates that the solubility of madecassoside is more complicated than that of asiaticoside, with the additional 6-OH.

3.2. Induction Period of Madecassoside. As the solubility of madecassoside in pure methanol is 0.0013826 (4.2191 g madecassoside/100 g methanol) at 298.15 K, a certain amount of madecassoside dissolved in methanol (4 g madecassoside/100 g methanol) was taken on for each test. Table 3 shows the x_m and S in dependence of the amount of

Table 3. S of Madecassoside in Different Methanol + Water Mixtures

x_m	S
0.0588	1.0511
0.1942	1.9937
0.36	1.8863
0.5676	2.8158
0.6923	4.5122
0.8351	7.2852

added water. However, the laser signal has no significant change during 6 h stirring, meaning that the induction period of madecassoside in all tested conditions is longer than 21 600 s, which is much longer than that of asiaticoside.

3.3. Induction Period of Asiaticoside. Figure 7 illustrates the experimental data of induction period obtained at various reagent compositions of methanol and water at 298.15 K. The results show that the induction period exponentially decrease with an increase in content of water except for x_m = 0.0588, which is longer than 0.6923. In addition, increasing the supersaturation accelerates the rate of nuclei formation and shortens the induction period.

3.4. Interfacial Tension. The plots of ln t_{ind} against $\ln^{-2} S$ at different methanol–water compositions are shown in Figure 8. They are all straight lines, and the correlation coefficients of the results are all larger than 0.95. The slopes of each line are also listed in Table 4. According to the results, x_m = 0.0588 and 0.8351 have the largest slope followed by x_m = 0.1942 and 0.6923, while x_m = 0.1942 and 0.6923 is the smallest.

The interfacial tension data at different methanol–water compositions are calculated by eq 6 (where V_m of asiaticoside is

dx.doi.org/10.1021/je300883a | J. Chem. Eng. Data 2012, 57, 3258–3263

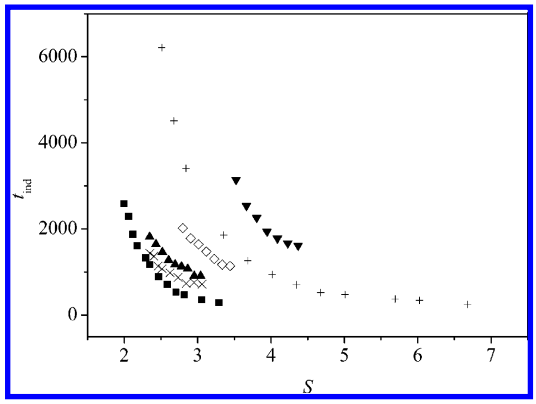

Figure 7. Induction period t_{ind} data of asiaticoside in different methanol + water mixtures (x_m, methanol mole content) as a function of supersaturation ratio S. +, x_m = 0.0588; ■, x_m = 0.1942; ×, x_m = 0.36; ▲, x_m = 0.5676; ◊, x_m = 0.6923; ▼, x_m = 0.8351.

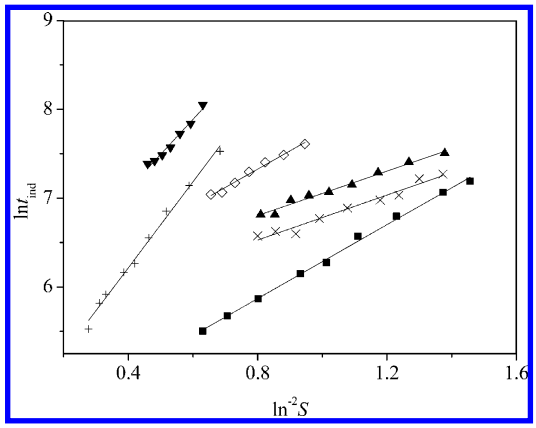

Figure 8. Linear regression of induction period t_{ind} data of asiaticoside at different methanol mole fractions x_m as a function of $\ln^{-2} S$. +, x_m = 0.0588; ■, x_m = 0.1942; ×, x_m = 0.36; ▲, x_m = 0.5676; ◊, x_m = 0.6923; ▼, x_m = 0.8351.

Table 4. Linear Regression Parameter of Induction Period Data of Asiaticoside

x_m	α
0.0588	4.84257
0.1942	2.08032
0.36	1.26922
0.5676	1.25088
0.6923	1.96767
0.8351	3.94456

5602.3 Å^3)[34] and illustrated in Figure 9. It can be seen that the obtained interfacial tension is in the range of (0.55 to 0.86) mJ·m^{-2}.

The interfacial tension values estimated in this study are compared with literature data as listed in Table 5. The interfacial tension values of asiaticoside are much smaller than those of its salts formed with vaterite, calcite, L-arginine phosphate, and dexamethasone sodium phosphate. This implies that the crystallization of the pure compound is much more difficult than for the salts mentioned above. Due to this reason, pentacyclic triterpenoid saponins mainly exist as noncrystalline powder.

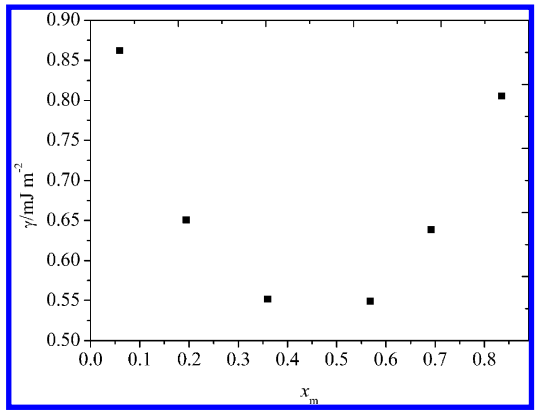

Figure 9. Interfacial tension γ data of asiaticoside in different methanol + water mixtures as a function of methanol mole fraction x_m.

Table 5. Interfacial Tension of Asiaticoside Compared to Other Compounds

solute	solution	interfacial tension mJ·m^{-2}
calcite[13]	ethylene glycol−water	21.2 to 41.5
L-arginine phosphate[35]	water	2.5 to 5.0
dexamethasone sodium phosphate[14]	methanol−acetone	3.5 to 9
asiaticoside	methanol−water	0.55 to 0.86

4. CONCLUSION

The solubilities of madecassoside in a mixture of methanol + water were determined in the temperature range from (298.15 to 328.15) K by a static−analytical method. The results indicate that the solubilities of madecassoside are quite similar to those of asiaticoside in the mixture of methanol−water mixture except at high water content and high temperature. The induction periods of asiaticoside and madecassoside in a mixture of methanol + water were determined at 298.15 K, which was carried out by a laser scattering method. Although these two compounds with the only difference of 6-OH have similar solubilities, they exhibit a quite different crystallization property that the induction period of madecassoside is at least 10 times longer than that of asiaticoside. Moreover, the interfacial tension data of asiaticoside were obtained, which are in the range of (0.55 to 0.86) mJ·m^{-2}.

AUTHOR INFORMATION

Corresponding Author

*Tel./Fax: +86-571-87952683. E-mail address: jiefu@zju.edu.cn (J.F.). Tel./Fax: +86-571-87952683. E-mail: luxiuyang@zju.edu.cn (X.-Y.L.).

Funding

The authors gratefully acknowledge the financial support by National Natural Science Foundation of China (No. 21176218, 20976160) and Zhejiang Key Innovation Team of Green Pharmaceutical Technology (Project No.: 2010R50043).

Notes

The authors declare no competing financial interest.

REFERENCES

(1) Vekilov, P. G. Nucleation. *Cryst. Growth Des.* **2010**, *10*, 5007−5019.

(2) Revalor, E.; Hammadi, Z.; Astier, J.; Grossier, R.; Garcia, E.; Hoff, C.; Furuta, K.; Okustu, T.; Morin, R.; Veesler, S. Usual and unusual crystallization from solution. *J. Cryst. Growth* **2010**, *312*, 939−946.
(3) Mullin, J. W. *Crystallization*; Butterworth-Heinemann: Oxford, 2001.
(4) Lu, X. Y.; Zheng, X. F. High-purity asiaticoside by solvent crystallization. CN Patent 101,407,536, 2009.
(5) Jia, G. T.; Lu, X. Y. Enrichment and purification of madecassoside and asiaticoside from Centella asiatica extracts with macroporous resins. *J. Chromatogr., A* **2008**, *1193*, 136−141.
(6) Lu, X. Y.; Jia, G. T.; Zheng, X. F. Preparation of Centella asiatica total triterpenoid saponins with macroporous resins. CN Patent 101,200,487, 2008.
(7) Zheng, X. F.; Lu, X. Y. Separation and structure determination of centellasaponin a and its isomer asiaticoside from Centella Asiatica total triterpenoid saponins. *J. Liq. Chromatogr. Relat. Technol.* **2011**, *34*, 1654−1663.
(8) Sönel, O.; Mullin, J. W. Interpretation of crystallization induction periods. *J. Colloid Interface Sci.* **1988**, *123*, 43−50.
(9) Boiteau, P.; Buzas, A.; Lederer, E.; Polonsky, J. Chemical constitution of asiaticoside. *Nature* **1949**, *163*, 258−258.
(10) Bontems, J. E. A new heteroside, asiaticoside, isolated from Hydrocotyle asiatica L. (Umbelliferae). *Bull. Sci. Pharmacol.* **1941**, *49*, 186−191.
(11) Xu, C. H.; Liu, D. J.; Chen, W. Effects of operating variables and additive on the induction period of $MgSO_4$-NaOH system. *J. Cryst. Growth* **2008**, *310*, 4138−4142.
(12) Tai, C. Y.; Chien, W. Effects of operating variables on the induction period of $CaCl_2$-Na_2CO_3 system. *J. Cryst. Growth* **2002**, *237−239* (Part 3), 2142−2147.
(13) Flaten, E. M.; Seiersten, M.; Andreassen, J. Induction time studies of calcium carbonate in ethylene glycol and water. *Chem. Eng. Res. Des.* **2010**, *88*, 1659−1668.
(14) Hao, H.; Wang, J.; Wang, Y. Determination of induction period and crystal growth mechanism of dexamethasone sodium phosphate in methanol-acetone system. *J. Cryst. Growth* **2005**, *274*, 545−549.
(15) Rajendran, K. V.; Rajasekaran, R.; Jayaraman, D.; Jayavel, R.; Ramasamy, P. Experimental determination of metastable zonewidth, induction period, interfacial energy and growth of non-linear optical-HFB single crystals. *Mater. Chem. Phys.* **2003**, *81*, 50−55.
(16) Liu, Y.; Wang, X.; Ching, C. B. Toward Further Understanding of Lysozyme Crystallization: Phase Diagram, Protein−Protein Interaction, Nucleation Kinetics, and Growth Kinetics. *Cryst. Growth Des.* **2010**, *10*, 548−558.
(17) Lundager Madsen, H. E. Theory of long induction periods. *J. Cryst. Growth* **1987**, *80*, 371−377.
(18) Haja Hameed, A. S.; Lan, C. W. Nucleation, growth and characterization of L-tartaric acid−nicotinamide NLO crystals. *J. Cryst. Growth* **2004**, *270*, 475−480.
(19) Söhnel, O.; Mullin, J. W. A method for the determination of precipitation induction periods. *J. Cryst. Growth* **1978**, *44*, 377−382.
(20) Söhnel, O.; Mullin, J. W. Precipitation of calcium carbonate. *J. Cryst. Growth* **1982**, *60*, 239−250.
(21) Kim, Y.; Hyung, W.; Haam, S.; Gun Shul, Y.; Koo, K. The effect of initial precipitates on the induction period of l-ornithine-l-aspartate during semi-batch drowning out crystallization. *J. Cryst. Growth* **2006**, *289*, 236−244.
(22) Lyczko, N.; Espitalier, F.; Louisnard, O.; Schwartzentruber, J. Effect of ultrasound on the induction time and the metastable zone widths of potassium sulphate. *Chem. Eng. J.* **2002**, *86*, 233−241.
(23) Kozlovskii, M. I.; Wakita, H.; Masuda, I. Analyses of precipitation processes of bis(dimethylglyoximato)Ni(II) and related complexes. *J. Cryst. Growth* **1983**, *61*, 377−382.
(24) Carosso, P. A.; Pelizzetti, E. A stopped-flow technique in fast precipitation kinetics—The case of barium sulphate. *J. Cryst. Growth* **1984**, *68*, 532−536.
(25) Kibalczyc, W.; Bondarczuk, K. Light scattering study of calcium phosphate precipitation. *J. Cryst. Growth* **1985**, *71*, 751−756.
(26) Gómez-Morales, J.; Torrent-Burgués, J.; Rodríguez-Clemente, R. Nucleation of calcium carbonate at different initial pH conditions. *J. Cryst. Growth* **1996**, *169*, 331−338.
(27) Kibalczyc, W.; Zielenkiewicz, A. Calorimetric investigations of calcium phosphate precipitation. *J. Cryst. Growth* **1987**, *82*, 733−736.
(28) Glasner, A.; Tassa, M. The thermal effects of nucleation and crystallization of KBr solutions: I. Experimental and mathematics, illustrated. *J. Cryst. Growth* **1972**, *13−14*, 441−444.
(29) Lu, L. L.; Lu, X. Y. Solubilities of Gallic Acid and Its Esters in Water. *J. Chem. Eng. Data* **2007**, *52*, 37−39.
(30) Lu, L. L.; Lu, X. Y. Solubilities of Polyhydroxybenzophenones in an Ethanol + Water Mixture from (293.15 to 343.15) K. *J. Chem. Eng. Data* **2008**, *53*, 1996−1998.
(31) Li, Y.; Lu, X. Y. Solubilities of Nizatidine in Water, Methanol, Ethanol, Acetone, and Ethyl Acetate from (273.15 to 343.15) K. *J. Chem. Eng. Data* **2010**, *55*, 4019−4020.
(32) Zheng, X. F.; Lu, X. Y. Measurement and Correlation of Solubilities of Asiaticoside in Water, Methanol, Ethanol, n-Propanol, n-Butanol, and a Methanol + Water Mixture from (278.15 to 343.15) K. *J. Chem. Eng. Data* **2011**, *56*, 674−677.
(33) Miyako, Y.; Zhao, Y.; Takeshima, K.; Kataoka, T.; Handa, T.; Pinal, R. Solubility of hydrophobic compounds in water−cosolvent mixtures: Relation of solubility with water−cosolvent interactions. *J. Pharm. Sci.* **2010**, *99*, 293−302.
(34) Mahato, S. B.; Sahu, N. P.; Luger, P.; Mueller, E. Stereochemistry of a triterpenoid trisaccharide from Centella asiatica. X-ray determination of the structure of asiaticoside. *J. Chem. Soc., Perkin Trans. 2* **1987**, *10*, 1509−1515.
(35) Arunmozhi, G.; Jayavel, R.; Subramanian, C. Experimental determination of metastable zone width, induction period and interfacial energy of LAP family crystals. *J. Cryst. Growth* **1997**, *178*, 387−392.